DERIVATION OF LIVE LOAD DISTRIBUTION FACTORS FOR SPREAD SLAB BEAM BRIDGES

Tevfik Terzioglu, PhD, Texas A&M Transportation Institute, College Station, TX
Mary Beth D. Hueste, PhD, PE, Zachry Dept. of Civil Eng., College Station, TX
John B. Mander, PhD, Zachry Dept. of Civil Engineering, College Station, TX

ABSTRACT

This paper presents an evaluation of a new prestressed concrete bridge type, spread slab beam bridges, in terms of performance and provides design guidelines including live load distribution factors (LLDFs). The new proposed bridge system offers an effective solution for short span bridges in low clearance areas where standard TxDOT slab beams are spaced apart, using a similar concept as spread box beam bridges. A challenging geometry with a wide beam spacing was constructed as a full-scale bridge and tested under static and dynamic vehicular loads to assess constructability and in-service performance. The measured response of the bridge during static and dynamic live load tests was used to verify the finite element method (FEM) modeling approach. Thirty-one spread slab beam bridge geometries were modeled using FEM to investigate an array of possible bridge geometries. Based on these FEM models, shear and moment LLDFs were derived for the design of spread slab beam bridges. The AASHTO Load and Resistance Factor Design (LRFD) spread box beam bridge LLDFs were also reviewed and they range from being unconservative to very conservative when applied to spread slab beam bridges. Unique LLDF expressions were developed for spread slab beam bridges to provide an appropriate estimate of load sharing for girder design.

Keywords: Precast Prestressed Concrete, Bridge Girder, Spread Slab Beam Bridge, Live Load Distribution Factor

INTRODUCTION

Slab-on-girder bridges are typically constructed by seating the precast prestressed girders on bearing pads on the bridge piers or abutments and then casting a concrete deck on top of the girders. The Texas Department of Transportation (TxDOT) often uses prestressed concrete slab beam bridges for short span bridges up to approximately 50 ft, especially for low clearance areas. The conventional approach consists of placing the slab beams side-by-side and casting a 5 in. thick CIP reinforced concrete deck on top of the slab beams (Fig. 1b). However, conventional slab beam bridges are more expensive compared to standard I-girder bridges, which are constructed using PCPs as stay-in-place formwork between girders.

One approach to reduce the number of girder lines is to modify the current short span bridge design that uses immediately adjacent precast prestressed concrete slab beams. The proposed solution is to spread out the slab beams and to use a conventional topped panelized deck as shown in Fig. 1a. It is anticipated that the use of spread slab beam bridges will result in a possible reduction in the overall bridge cost while providing another design alternative for short span bridges.

For spread slab beam construction, the moments and shears imposed by eccentrically located truck loads will differ in the individual slab beams across the overall bridge deck cross-section. Appropriate girder live load distribution factor (LLDF) formulas for this case are not available in the AASHTO Load and Resistance Factor Design (LRFD) Bridge Design Specifications[1] and need to be investigated. While this study aims to evaluate the potential of the proposed spread slab beam deck configuration, the principal research focus is directed toward developing design recommendations for this bridge type, with a particular emphasis on establishing appropriate LLDFs for this class of spread slab beam bridges.

A full-scale 46 ft-7 in. long, and 34 ft wide spread slab beam bridge was constructed and field tested at the Texas A&M University Riverside Campus. The measured response was then used to validate the finite element method (FEM) and grillage analysis modeling techniques to evaluate the accuracy of alternative computational methods for modeling spread slab beam bridges. Finally various bridge geometries with total bridge spans between 31–51 ft and beam spacings from 6.5 ft to 11 ft (center-to-center) were modeled using the finite element method, and investigated to evaluate their LLDFs.

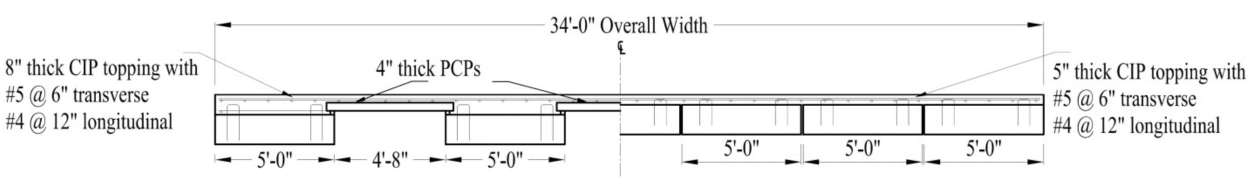

(a) Spread slab beam bridge (b) Conventional slab beam bridge

Fig. 1 Prestressed concrete slab beam bridges

The complexity of calculating the design moment and shear actions for an individual bridge girder under imposed live loads necessitates simplified analysis methods. The design moment and shear demands for an individual bridge girder depend on various parameters such as the position of the load, the girder spacing, the span length, and the relative deck-to-girder stiffness. In order to simplify the design process, a longstanding methodology has evolved whereby a multiple girder bridge deck can be simplified to consider the structure to be one-girder line or beam element for design. Thus, live load distribution factors are applied to convert the design live load into the forces to design one girder and its associated deck slab.

The concept of live load distribution factors was first developed based on the studies conducted by Westergaard[2] and Newmark[3] and adopted in the first edition of AASHO Standard Specifications[4] in 1931. These early formulas, which are also called *S/D* equations, were used by all AASHTO Standard Specifications[5] until the 17th edition in 2002 with slight modification over the years. Although simple *S/D* equations were overly conservative for many bridge geometries, they tended to generate reasonably accurate results for girder spacings around 6 ft and bridge spans around 60 ft. These equations were valid for normal bridges (girders perpendicular to abutments) and for simply supported spans[6]. After the 1950s most of the modern highway bridges began to have longer spans, skewed supports, curved alignments, and continuous interior piers. As the demand for new and challenging bridge superstructures increased, researchers raised the question about the accuracy of the *S/D* equations and have studied their applicability and suggested new equations for many cases[7-10].

The LLDF equations provided in AASHTO LRFD Specifications[1] were first introduced in the first edition of the AASHTO LRFD Bridge Design Specifications[11] and have not been updated since then. These LLDF equations were developed by Zokaie et al.[6] as part of NCHRP research project 1226 and cover a wide range of bridge types and geometries. While these updated LLDF equations are also simplified, they consistently provided conservative results for the bridges within the specified range of bridge geometries[12, 13]. Although the new proposed LLDF expressions provide reasonable results for many common bridge types and geometries, they have limited ranges of applicability and are relatively more complicated. Many researchers proposed simplified expressions, studied different ranges of applicability, and included models for dynamic amplification and multiple presence factors[14-16].

The objective of the study described in this paper is the empirical derivation of live load distribution factors for the interior and exterior girders of spread slab beam bridges for span lengths within the range of 31 to 51 ft. The proposed LLDF expressions were derived by analyzing 31 bridge models using FEM, with each bridge model having different geometries. Proposed equations were obtained using a methodology similar to that adopted for developing the LLDF equations found in the AASHTO LRFD Bridge Design Specifications[1]. The parameters for the equations were chosen based on similar formulas used for spread box beam bridges in the current AASHTO LRFD Specifications[1]. FEM analyses were used to determine the effect of the chosen parameters, which are span length, beam spacing, and beam depth. Additional details for this study were documented by Hueste et al.[17]

SUMMARY OF DESIGN APPROACH AND EXPERIMENTAL RESULTS

The research approach in this study included three major phases: (1) parametric study to identify possible benefits of the new spread slab beam bridge system and achievable design space based on the AASHTO LRFD Bridge Design Specifications[1]; (2) construction and field testing of a full-scale bridge selected from the parametric study; and (3) derivation of LLDFs to determine moment and shear demands for spread slab beam systems.

PARAMETRIC STUDY

A detailed parametric study was conducted to develop various designs for alternative parameters and geometries. A total of 44 bridges were designed considering four standard TxDOT slab beam types (12 in. or 15 in. deep with a 4 ft or 5 ft width), five different bridge widths (26 ft, 30 ft, 34 ft, 40 ft, and 46 ft) and beam spacings varying from 6.5 ft to 11.5 ft.

Each slab beam was designed based on a given number of strands unlike typical design procedures where the girders are designed for a given span length. The objective is to determine the span length design space for each specific bridge geometry for a given number of strands. This provides a more complete picture in terms of the applicable range of the considered geometric parameters. Initially, all strand locations were considered to be filled (44 strands for 4 ft wide slab beams and 56 strands for 5 ft wide slab beams) and then two strands were subtracted at each step until the section reached the cracking limit. The maximum achievable span lengths were determined for eight different AASHTO LRFD limit states including allowable tension and compression stress limits at release, at the time of deck placement, and at service; ultimate flexural strength; and the deflection limit at service. The AASHTO HL-93 live load model was adopted as the vehicle loading and AASHTO LRFD[1] spread box beam LLDFs were used for the parametric study.

Fig. 2 shows the achievable span length solutions for all eight limit states for select bridge geometries. Each curve represents an upper bound span length solution for the limit state considered. The release limit corresponds to the upper bound for the allowable compression or tension stress limit (whichever governs) at release when no strands are debonded. The debonded release limit is the upper bound when some strands are debonded up to 6 ft for 15 in. deep slab beams or up to 9 ft (or $0.2L$ for beams shorter than 45 ft) for 12 in. deep slab beams. For all the analyzed cases, the tension stress limit at service and the tension stress limit at release (with debonding) control the solution domain. The yellow shaded region shows the feasible solution domain and the red checkmark is the maximum achievable span. More detailed information about the parametric study, shear design checks, and the constructability of spread slab beam bridges can be found in Terzioglu et al.[18, 19].

FIELD TESTING OF FULL-SCALE RIVERSIDE BRIDGE

One of the main objectives of this research project was to identify moment and shear LLDFs for spread slab beam bridges. The experimental part of the research project consisted of building a full-scale spread slab beam bridge and testing it under service loads in order to assess the constructability and serviceability of the bridge, and to study live load distribution factors. For that purpose, one of the challenging geometries identified during the parametric study was selected and built at the edge of a runway located at the Texas A&M University Riverside Campus. The spread slab beam bridge has a 46 ft 7 in. span length, with a total width of 34 ft. The minimum deck thickness is 8 in. between slab beams.

Fig. 3 shows the photographs of the load cells at the supports and construction process of the superstructure components. The bridge superstructure is composed of four slab beam girders spaced at 9 ft 8 in. apart, PCPs that span between girders as stay-in-place forms, and a CIP reinforced concrete deck that combines all the precast elements and creates the monolithic bridge superstructure.

	S=7.00–7.20 ft	*S*=8.67–8.75 ft	*S*=10.00–10.25 ft
4SB12	(a) 40 ft Wide with 6 Beams	(b) 30 ft Wide with 4 Beams	(c) 34 ft Wide with 4 Beams
4SB15	(d) 40 ft Wide with 6 Beams	(e) 30 ft Wide with 4 Beams	(f) 34 ft Wide with 4 Beams
5SB12	(g) 34 ft Wide with 5 Beams	(h) 40 ft Wide with 5 Beams	(i) 46 ft Wide with 5 Beams
5SB15	(j) 34 ft Wide with 5 Beams	(k) 40 ft Wide with 5 Beams	(l) 46 ft Wide with 5 Beams

Service Tension; Casting Tension; Ultimate Strength; Release Limit
Service Compression; Casting Compression; Deflection; Debonded Release Limit

Fig. 2 Span length solution domain for select bridge geometries

(a) South-end load cell assembly and layout

(b) Slab beam placement

(c) CIP deck and approach slab

Fig. 3 Construction of the full-scale spread slab beam bridge – Riverside Bridge

All four girders of the bridge were heavily instrumented to capture deflection profiles, mid-span strains, support reactions, and natural frequencies. A total of 16 load cells were placed at both ends of each slab beam to determine the load sharing between slab beams under vehicle loading and the corresponding shear distribution factors. The moments for each girder were calculated from the deflection profiles of the slab beams as well as from the strain gage measurements. In order to be able to capture natural frequency and mode shapes of the girders during dynamic testing, a total of eight accelerometers were attached on the bottom of the slab beams. Five accelerometers were attached along one of the interior beams, and the remaining three accelerometers were attached at the midspan locations of each of the other slab beams.

The bridge was tested under static and dynamic service loads using two different trucks, a dump truck and a water tanker, at various transverse and longitudinal positions to create critical load configurations for shear and moment. Fig. 4 shows a photo taken during a full speed testing of the bridge using a loaded dump truck.

Fig. 4 Vehicle testing at in-service speeds (around 40 mph)

Fig. 6 shows the deflection profiles of all four slab beams obtained from the string potentiometer measurements. The moments at the midspan of each beam for the moment critical position of the vehicles were obtained using the deflection profile from seven string potentiometers that were clustered at the center of the beams. A third-order polynomial was fit through the deflection curve. The moment at midspan was then calculated using the curvature at midspan and multiplying it by EI, where E is the modulus of elasticity and I is the moment of inertia. Moments at midspan were also calculated using strain values obtained from strain gages.

Fig. 5 shows the four transverse positions of the vehicles during the static and dynamic testing of the bridge. The maximum deflection of 0.12 in. was observed at Beam 4 when the vehicle was located at the center of Alignment 1. The deflection profiles changed as the vehicle moved transversely. Maximum deflections were observed for Beam 4 when the vehicle was at Alignment 1 and Alignment 3.

The moment reactions and moment distribution factors calculated using two different measurements (string potentiometers and strain gages) were plotted and are compared in Fig. 7. The critical moment distribution factors are obtained when both lanes are loaded for a two-lane bridge. Therefore, the results of two different alignments were superimposed to obtain two-lane-loaded results. Alignment 1+2 and Alignment 3+4 were already defined as alignment couples that allow two trucks traveling as close as possible to each other.

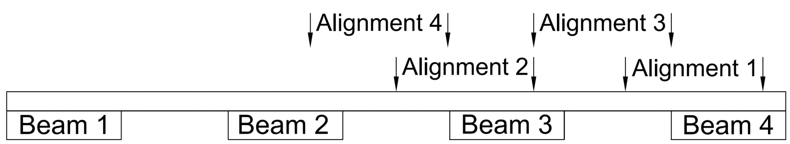

Fig. 5 Transverse alignments for static and dynamic testing

(a) Alignment 1 (b) Alignment 2

(c) Alignment 3 (d) Alignment 4

Fig. 6 Deflection profiles for dump truck loading

The results indicate that the moment values obtained using strain gage data are slightly higher than those calculated using string potentiometer measurements. However, the moment LLDF values are similar for the two different measurement methods and provide consistent results. The maximum moment LLDFs recorded due to the dump truck loading are 0.65 for an interior beam and 0.72 for an exterior beam when Alignment 1+2 is loaded.

Fig. 8 shows both static and amplified north support reactions due to dynamic impact. Reaction data recorded during the dynamic tests were analyzed and compared to the static data. For the dynamic tests, the dump truck was driven at a speed of 40 mph along the same four transverse alignments used for the static tests. For all the dynamic tests, vehicles were driven from south to north. The dynamic amplification at the north support was prominent when the dump truck was driven along Alignment 2. The amplification was about 37 percent for Beam 3. This is larger than the standard 33 percent increase for impact specified by the

AASHTO LRFD Specifications. More detailed information about experimental results, different vehicle loadings, and load distribution factors can be found in [17], Terzioglu et al.[20].

COMPUTATIONAL MODELING OF THE RIVERSIDE BRIDGE

The experimental results obtained from the field testing of the Riverside Bridge were used to investigate different modeling approaches including the grillage method and the FEM. Moment and shear predictions from these computational models were compared with experimentally obtained results. The FEM modeling approach providing the best agreement with the experimental results was used to develop additional FEM models having varying geometries to investigate the effect of different parameters. These models then utilized for further investigation in the parametric study for deriving moment and shear LLDF formulas.

(a) Moments for Alignment 1&2 (b) Moment LLDFs for Alignment 1&2

(c) Moments for Alignment 3&4 (d) Moment LLDFs for Alignment 3&4

Note: SP = String Potentiometer, SG = Strain Gage

Fig. 7 Midspan moments and moment LLDFs for dump truck loading

(a) Reactions for Alignment 1+2 (b) Reactions for Alignment 3+4

Fig. 8 North support reactions for dump truck loading

Grillage analysis is historically the most basic type of computational modeling technique for analyzing slab and beam bridges. This method idealizes the bridge superstructure by assuming that it may be represented by a mesh of frame elements in each of the two orthogonal directions. This assumption reduces the real structure to a 2D plane of grillage elements where longitudinal members represent composite T-beams, composed of slab beams with their associated slab width, and transverse members represent the slab only. Although this method provides sufficiently accurate predictions, it requires more time for modeling the elastic parameters and loading arrangement correctly as compared to current available FEM software with modern user-friendly graphical interfaces.

A 3D finite element model that uses solid brick elements enables representation of the correct bridge geometry including the vertical positions of the boundary conditions. Two different commercial FEM analysis programs were utilized to compare analysis accuracy: (1) Abaqus[21], a general purpose program for solving a broad range of engineering problems, and (2) CSiBridge[22], a program more specific to bridge engineering.

The experimentally observed deflections were compared to those predicted by the two commercial FEM programs. Fig. 9 shows the comparison of deflection values for two of the four truck wheel alignments tested for the Riverside Bridge. It shows that both FEM models can predict the deflection profiles reasonably well. The maximum difference between the measured and predicted deflections is 0.010 in. for Abaqus and 0.012 in. for CSiBridge. It should be noted that the string potentiometers measurements are within a 0.005 in. resolution.

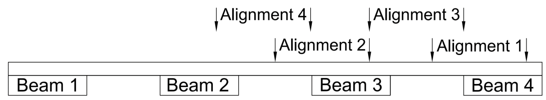

(a) Transverse positions of the wheel alignments

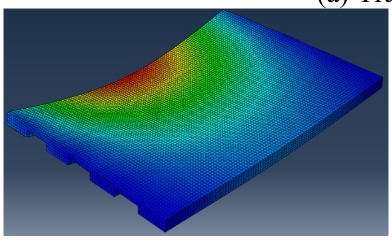

(b) Deflection profiles – Alignment 1

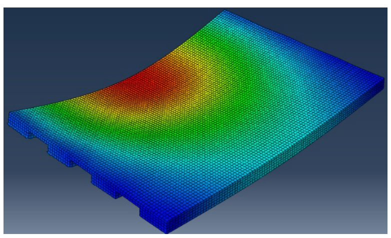

(c) Deflection profiles – Alignment 3

Fig. 9 Comparison of deflection fields with the experimental results

Maximum moment and shear responses of each slab beam for moment and shear critical longitudinal positions of the dump truck used for testing were estimated using grillage and FEM models. The lateral distribution of live loads between girders was then calculated from these moment and shear estimates. The maximum of these responses controls the design of an interior or exterior beam. These maximum values are plotted as bar charts in Fig. 10 and Fig. 11 for moment and shear results to visually inspect the accuracy of the computational methods. It is evident that the grillage model provides slightly conservative estimates for critical moment results, whereas the FEM model estimates for moments are slightly unconservative. Shear predictions obtained from both FEM programs and grillage analysis are in close agreement (within 5 percent) with the test results for most of the maximum shear cases.

(a) Interior Moment (b) Exterior Moment (c) Int. Moment LLDFs (d) Ext. Mom. LLDFs

Fig. 10 Comparison of critical moment results

(a) Interior Shear (b) Exterior Shear (c) Interior Shear LLDFs (d) Ext. Shear LLDFs

Fig. 11 Comparison of critical north support shear actions

METHODOLOGY FOR DEVELOPING LIVE LOAD DISTRIBUTION FACTORS

LLDF formulas were developed following the same procedure used by Zokaie et al.[6] for the AASHTO LRFD Specifications[1]. Several assumptions were made to simplify the procedure.

- The effect of each parameter on the LLDF can be modeled using a power function of the general form, where *x* is the parameter under consideration, and are the coefficients that are determined by nonlinear least squares regression.
- The considered parameters were assumed to be independent from each other

After defining the separate effect of each parameter with a power curve, the combined effect was modeled by multiplying those power terms with a combined coefficient as follows:

12* MERGEFORMAT ()

where the coefficient was determined after all the powers (, ,) were established. All three power coefficients were determined by studying each parameter separately. Then the common coefficient of the final expression () was calculated as:

34* MERGEFORMAT ()

The approach outlined below was followed to derive LLDFs for moment and shear in interior and exterior beams, including one-lane-loaded and multiple-lane-loaded cases

1. A number of bridges were designed and modeled using the FEM, specifically with the CSiBridge software. The AASHTO LRFD HL-93 design truck loads were placed in numerous transverse and longitudinal locations to obtain the most adverse combination for maximizing moment and shear in the interior and exterior slab beams. Thus, for each bridge a matrix of LLDFs was calculated and tabulated by group types.
2. For each bridge within a specific grouping, all parameters (except one) were held constant, and a log-log graph of LLDF versus the key variable was plotted. A nonlinear least square best fit was found for the form, where in particular the parameter (the slope of the log-log plot) was obtained, plotted, and recorded.
3. Once all results for the power indices were found, the value of for the i^{th} bridge was determined using Eqn. (2)
4. Collectively, when all values of were plotted they formed a lognormal distribution for which the median of allvalues (that is the geometric mean, or 50^{th} percentile) gives the overall "best fit" for all bridges, and the lognormal standard deviation describes the dispersion in the load demand actions.
5. Formulas were grouped by type, such as moments, shears, one-lane cases, and multiple-lane cases.
6. A reexamination of the resulting empirical formulas from Step 5 was made and then rationally adjusted to provide revised LLDFs that are more compatible with the companion AASHTO LRFD LLDF formulas[1]. The coefficients were adjusted so that there is approximately a non-exceedance probability of 5 percent (lognormal minus 1.65 lognormal standard deviations), and the final empirical design LLDF formulas are mostly conservative (i.e., 95 percent likelihood of being conservative).

REGRESSION MODEL OF EMPIRICAL LLDF RESULTS

The effect of each chosen key parameter (span length, beam spacing, and beam depth), on live load distribution factors was investigated. Live load distribution factors for all eight formulas (moment and shear in interior and exterior beams for one-lane-loaded and multiple-lane-loaded cases), for each girder, and for each of the 31 bridge geometries were obtained from the FEM models and used for developing the empirical LLDFs for design applications. The maximum moment and shear values for interior and exterior girders were obtained from the FEM analysis. These moment and shear forces for one-, two-, and three-lane-loaded cases were multiplied with the AASHTO LRFD multiple presence factors of 1.2, 1.0, and 0.85, respectively. Then the LLDFs for all eight formulas were calculated by dividing the maximum moment (or shear value) with the moment (or shear value) of an isolated simply supported beam having the same span length.

SENSITIVITY OF LLDF TO SPAN LENGTH, *L*

Fig. 12 presents the variation of LLDFs with respect to span length, , which is one of the most important parameters influencing the load distribution between girders. In order to evaluate the effect of changing span length, all other parameters were kept constant and the span length was changed between 29 ft 7 in. to 45 ft 7 in. for a total of seven different bridge spans. The LLDF values were plotted on a log-log graph to provide visual examination of the effect of the span length on the LLDFs.

(a) Interior Beam Moment LLDF (b) Exterior Beam Moment LLDF

(c) Interior Beam Shear LLDF (d) Exterior Beam Shear LLDF

Fig. 12 Effect of span length on live load distribution factors

SENSITIVITY OF LLDF TO BEAM SPACING, *S*

Fig. 13 depicts in log-log space the sensitivity of beam spacing,, on LLDFs. Beam spacing is the most important parameter that effects the variation of the LLDFs. A total of 11 superstructure geometries were modeled to evaluate the variation of LLDFs with beam spacing. The investigation of the effect of beam spacing on LLDFs revealed that the relationship between beam spacing and LLDFs was more prominent as compared to span length and beam depth.

(a) Interior Beam Moment LLDF (b) Exterior Beam Moment LLDF

(c) Interior Beam Shear LLDF (d) Exterior Beam Shear LLDF

Fig. 13 Effect of beam spacing on live load distribution factors

SENSITIVITY OF LLDF TO BEAM DEPTH,

Fig. 14 shows how variation in beam depth,, affects the LLDFs. Although there are only two different standard slab beam depths used in practice by TxDOT, 12 in. and 15 in., seven different beam depths were analyzed to develop more data points to fit a power curve and gain a better understanding of the effect of beam depth. A total of seven hypothetical beam depths between 12 in. to 21 in. were introduced, and seven bridge superstructure geometries were modeled for investigating the influence of beam depth on LLDFs. As discussed earlier, beam depth somewhat affects the LLDFs but is not as prominent as beam spacing and span length. An investigation of the graphs for the sensitivity of beam depth shows that the LLDF values for shear in an exterior beam are not sensitive to the beam depth. The slopes of these curves are almost zero.

(a) Interior Beam Moment LLDF (b) Exterior Beam Moment LLDF

(c) Interior Beam Shear LLDF (d) Exterior Beam Shear LLDF

Fig. 14 Effect of beam depth on live load distribution factors

DERIVATION OF LLDF EQUATIONS

Live load distribution factors obtained from each one of the 31 bridge superstructures for all eight LLDF categories (moment and shear in interior and exterior beams for one-lane-loaded and multiple-lane-loaded cases) were calculated using the moment and shear results from FEM models. These FEM values were then compared with those obtained from the AASHTO LRFD Specifications[1] spread box beam formulas, theoretical least square (LS) best fit LLDF equations, and new proposed LLDF equations.

For a given bridge superstructure, the coefficient was calculated using Eqn. (2), which resulted in 31 different coefficients that are close but slightly different from each other. The median (average of values) of these coefficients was used as an initial estimate, while the lognormal standard deviation,, was used as a measure of scatter of the results. The final coefficient for that specific LLDF case was calculated to minimize the lognormal standard deviation,. This procedure was repeated for all eight categories for calculating the coefficients of the empirical LLDF equations.

In order to derive LLDF formulas that are similar to those in the AASHTO LRFD Specifications[1] for spread box beams, the powers of the parameters were kept the same or as similar as reasonable to ensure remained close to the theoretical equation. For the other cases where using the same power gives higher values, the powers were chosen based on the theoretical power values and the format of the AASHTO LRFD Specifications[1] spread box beam formulas. The principal proposed coefficient was increased by accepting a 5 percent exceedance criterion, which means that up to 5 percent of the cases analyzed were permitted to be unconservative (smaller) compared to the more accurate FEM-based LLDF values. All eight proposed LLDF formulas for moment and shear are listed in Table 1.

LLDFs obtained from the FEM analysis were compared with those calculated from the AASHTO LRFD Specifications[1] spread box beam equations, the LS best fit theoretical equations, and the proposed LLDF equations for design. The comparison of these three LLDF equations versus FEM results is shown in the graphs provided in Fig. 15 and Fig. 16. These figures provide plots of the moment and shear LLDF comparison with more accurate FEM values for all 31 bridges. Therefore, the LLDFs obtained from theoretical equations, new proposed equations, and the AASHTO LRFD Specifications[1] spread box beam formulas are compared to the FEM-based LLDFs. Each data point on the graphs represents an LLDF for a specific category. The cumulative probabilities of the LLDF ratios (Theory/FEM, Proposed/FEM, and AASHTO/FEM) are plotted to better visualize the distribution of each data point and their probability of occurrence. The solid red line in these figures represents the lognormal model curve for the proposed equation. The model curve is a lognormal curve that has the same lognormal standard deviation and median as the ratios of the proposed equation.

Table 1 Approximate LLDF equations for spread slab beam bridges

			No.	AASHTO Spread Box Beam Formulas	Least Square Best Fit Relations	Proposed LLDF Design Equations
Moment LLDF	Interior Beam	One Lane Loaded	1			
		Multiple Lanes Loaded	2			
	Exterior Beam	One Lane Loaded	3	Lever Rule		
		Multiple Lanes Loaded	4			
Shear LLDF	Interior Beam	One Lane Loaded	5			
		Multiple Lanes Loaded	6			
	Exterior Beam	One Lane Loaded	7	Lever Rule		
		Multiple Lanes Loaded	8			

Range of Applicability for Proposed LLDF Design Equations:
31 ft $\leq L \leq$ 51 ft, 6.5 ft $\leq S \leq$ 11 ft, 12 in. $\leq d \leq$ 21 in.

In the case of the one-lane-loaded moment in interior beams (Fig. 15a), a majority of the LLDF results calculated using the AASHTO LRFD Specifications[1] formula are unconservative when compared to the exact FEM LDFs. Hence a new LLDF equation, which results in a slightly conservative LLDF values was introduced. Fig. 15b shows the comparative graphs for the multiple-lane-loaded moment in interior beams. The AASHTO LRFD Specifications[1] formulas are slightly higher than the FEM values. Therefore, the spread box beam formula for the multiple-lane-loaded moment in interior beams was kept the same.

Fig. 15c and 15d show cumulative probabilities for both one-lane- and multiple-lane-loaded shear LLDF results in interior beams. The results indicate that the AASHTO LRFD Specifications[1] LLDFs are unconservative for both one-lane-loaded and multiple-lane-loaded cases. This finding is consistent with LLDFs calculated from the experimentally measured shear values. Therefore, new shear LLDF equations are introduced that give slightly higher LLDFs. The parameters in the new shear LLDF equations were rearranged to be similar to the AASHTO LRFD Specifications[1] spread box beam formulas.

(a) One-lane-loaded – moment LLDF (b) Multiple-lane-loaded – moment LLDF

(c) One-lane-loaded – shear LLDF (d) Multiple-lane-loaded – shear LLDF

Fig. 15 Probability distributions of LLDF ratios (calculated/FEM) for interior beams

Fig. 16a and 16b show the comparative probability distributions for one-lane and multiple-lane-loaded moment LLDFs in exterior beams. The proposed equations give slightly conservative results for all considered 31 bridge models. Whereas, AASHTO LRFD Specifications[1] LLDFs results are overly conservative, by more than 50% in some cases. A new equation having a similar formulation as for the interior beam LLDFs is introduced instead of the lever rule.

Fig. 16c and d shows the comparative plots of all three LLDF equations for shear in exterior beams versus the FEM results. The AASHTO LRFD Specifications[1] spread box beam LLDF formulas are an average of 25 percent conservative for one-lane-loaded and more than 30 percent conservative for multiple-lane-loaded shear in exterior beams. The AASHTO LRFD Specifications[1] recommend using the lever rule for determining exterior girder shear for the one-lane-loaded case. However, the lever rule gives overly conservative shear LLDFs for the considered spread slab beam bridges. For the case of multiple-lane-loaded shear in exterior beams, the LLDF for shear is calculated by multiplying the interior beam shear LLDF by a coefficient that is a function of the distance of the exterior beam from the edge of the bridge. Again this approach gives very conservative results that are up to 50 percent conservative in some cases. Therefore new LLDF expressions were derived for both one-lane and multiple-lane-loaded categories, which results in slightly conservative LLDFs.

(a) One-lane-loaded moment LLDF (b) Multiple-lane-loaded moment LLDF

(c) One-lane-loaded shear LLDF (d) Multiple-lane-loaded shear LLDF

Fig. 16 Probability distributions of LLDF ratios (calculated/FEM) for exterior beams

CONCLUSIONS

An alternative bridge type, a spread slab beam bridge, has been developed as a potentially more economical option for short span bridges. This research investigated the potential of the spread slab beam bridge system, evaluated in-service performance, and developed design recommendations with a focus on appropriate relationships for live load distribution factors. Alternative analytical modeling approaches including the FEM and grillage method were evaluated. Live load distribution factors for spread slab beams were derived based on computational models representing the design space for this class of simply supported spread slab beam bridges. The LLDF equations were developed for key parameters including beam spacing (*S*), span length (*L*), and beam depth (*d*). The following conclusions were drawn based on this study.

1. Deflection predictions obtained from both commercial FEM software programs (Abaqus and CSiBridge) show good agreement with the experimental results.
2. Moment and shear LLDFs calculated from the moment and shear predictions of both FEM software programs were in a good agreement with the test results. When carefully developed, the grillage model also predicts moment and shear response quite accurately.
3. Although both grillage analysis and FEM models can be considered sufficiently accurate and could be used for further development of LLDFs, one should use the best available analysis tools.
4. Unique LLDF equations were developed for spread slab beam bridges to provide an appropriate level of conservatism. The new proposed equations produce slightly conservative results for 95% of the considered models for all LLDF categories when compared with the LLDFs calculated from FEM analysis.
5. Common TxDOT practice for precast prestressed concrete bridges is to design all the girders for the same forces as an interior girder in order to take into account possible future widening of the bridge. Therefore, all girders are designed based on the maximum interior girder shear and moment demands, unless the exterior demands are greater. The two governing proposed LLDF equations for an interior girder for the multiple-lanes-loaded case are:

   For moments:

   For shear:

   where 31 ft $\leq L \leq$ 51 ft; 6.5 ft $\leq S \leq$ 11 ft; 12 in. $\leq d \leq$ 21 in.
6. The AASHTO LRFD spread box beam LLDF equations were reviewed for their applicability to spread slab beam bridges.
   a. The AASHTO LRFD LLDF expressions resulted in unconservative predictions for interior beams in spread slab beam bridges; except for the multiple-lane-loaded moment LLDF, which was kept the same for spread slab beam bridges.
   b. The AASHTO LRFD LLDF expressions gave overly conservative results for exterior beams in spread slab beam bridges.

REFERENCES

1. AASHTO, "AASHTO LRFD Bridge Design Specifications." 2012, *American Association of State Highway and Transportation Officials (AASHTO)*: Washington, DC.
2. Westergaard, H.M., "Computation of Stresses in Bridge Slabs due to Wheel Loads," *Public Roads*, 1930. 11(1): p. 1-23.
3. Newmark, N.M., "A Distribution Procedure for Analysis of Slabs Continuous over Flexible Beams." 1938, *University of Illinois*: Urbana, IL.
4. AASHO, "Standard Specifications for Highway Bridges, 1st Edition." 1931, *American Association of State Highway Officials*: Washington, DC.
5. AASHTO, "Standard Specifications for Highway Bridges, 17th Edition." 2002, *American Association of State Highway and Transportation Officials*: Washington, DC.
6. Zokaie, T., R.A. Imbsen, and T.A. Osterkamp, "Distribution of Wheel Loads on Highway Bridges," in *NCHRP Project Report 12-26*. 1991, *Transportation Research Board*: Washington, DC.
7. Douglas, W.J. and D.A. Vanhorn, "Lateral Distribution of Static Loads in a Prestressed Concrete Box-Beam Bridge - Drehersville Bridge," in *Project 315*. 1966, *Fritz Engineering Laboratory, Department of Civil Engineering, Lehigh University*: Bethlehem, Pennsylvania.
8. Marx, H.J., N. Khachaturian, and W.L. Gamble, "Development of Design Criteria for Simply Supporter Skew Slab-and-Girder Bridges." 1986, *University of Illinois at Urbana-Champaign*.
9. Bakht, B. and F. Moses, "Lateral Distribution Factors for Highway Bridges," *Journal of Structural Engineering*, 1988. 114(8): p. 1785-1803.
10. Bishara, A.G., M.C. Liu, and N.D. El-Ali, "Wheel Load Distribution on Simply Supported Skew I-Beam Composite Bridges," *Journal of Structural Engineering*, 1993. 119(2): p. 399-419.
11. AASHTO, "AASHTO LRFD Bridge Design Specifications, 1st Edition." 1994, *American Association of State Highway and Transportation Officials, Customary US Units*: Washington, DC.
12. Nowak, A.S., "Live Load Model for Highway Bridges," *Structural Safety*, 1993. 13: p. 53-66.
13. Chen, Y. and A. Aswad, "Stretching Span Capability of Prestressed Concrete Bridges under AASHTO LRFD," *Journal of Bridge Engineering*, 1996. 1(3): p. 112-120.
14. Nowak, A.S., "Calibration of LRFD Bridge Code," *Journal of Structural Engineering*, 1995. 121(8): p. 1245.
15. Sotelino, E., J. Liu, W. Chung, and K. Phuvoravan, "Simplified Load Distribution Factor for Use in LRFD Design," *Joint Transportation Research Program*, 2004: p. 1-148.
16. Puckett, J.A., S.X. Huo, M. Jablin, and D.R. Mertz, "Framework for Simplified live load distribution-factor computations," *Journal of Bridge Engineering*, 2011. 16(6): p. 777-791.
17. Hueste, M.D., J.B. Mander, T. Terzioglu, D. Jiang, and J. Petersen-Gauthier, "Spread

Prestressed Concrete Slab Beam Bridges," in *Research Report No. FHWA/TX-14/0 6722-1*. 2015, *Texas A&M Transportation Institute and Texas Department of Transportation*.
18. Terzioglu, T., D. Jiang, M.B.D. Hueste, and J.B. Mander, "Design and Constructibility of Spread Slab Beam Bridges," ASCE *Journal of Bridge Engineering*, 2016: p. 04016089.
19. Terzioglu, T., "Behavior and Design of Spread Prestressed Concrete Slab Beam Bridges," in *Civil Engineering*. 2015, *Texas A&M University*: College Station. p. 406.
20. Terzioglu, T., D. Jiang, M.B.D. Hueste, J.B. Mander, and G.T. Fry, "Experimental Investigation of a Full-Scale Spread Slab Beam Bridge," ASCE *Journal of Bridge Engineering*, 2016: p. 04016082.
21. Dassault Systemes, S.A., "Abaqus, version 6. Abaqus, Inc." 2013: Providence, RI, USA.
22. Computers and Structures, I., "CSiBridge, Integrated 3-D Bridge Analysis, Design and Rating." 2015, *Computers and Structures, Inc.*: Berkeley, California, USA.